

IMPLEMENTATION OF SPREAD MASS MODEL OF ION HOSE INSTABILITY IN LAMDA *

Yan Tang, ATK-MR, Albuquerque, NM 87110

Thomas P. Hughes, Thomas C. Genoni, Voss Scientific, Albuquerque, NM 87108

Carl A. Ekdahl, Los Alamos National Laboratory, Los Alamos, NM 87545

Martin E. Schulze, SAIC, Martin E. Schulze, SAIC, San Diego, CA 92121

Abstract

The ion-hose instability sets limits on the allowable vacuum in the DARHT-2 linear induction accelerator (2kA, 18.6MeV, 2μs). Lamda is a transport code which advances the beam centroid and envelope in a linear induction accelerator from the injector to the final focus region. The code computes the effect of magnet misalignment, beam breakup instability, image-displacement instability, and gap voltage fluctuation. To support the experiments, we have implemented the SM model of ion-hose instability into Lamda. Unlike the ordinary SM ion-hose code which assumes the uniform axial magnetic field, Lamda ion-hose calculation includes varying axial magnetic field, accelerating beam, gas pressure file, varying beam radius, and elliptical beam. This paper describes the Lamda ion-hose instability code, the benchmarks against a semi-analytical SM code, and the particle-in-cell code Lsp. A prediction of ion-hose instability for a 2.5MeV-1.4kA beam in the DARHT-2 is also presented.

INTRODUCTION

The DARHT-2 linear induction accelerator is designed to produce a 2-kA, 20-MV, 2-μs flat-top electron beam with a small time-integrated spot-size on an x-ray converter target [1]. This requires excellent magnetic transport and control of the beam transverse instabilities. During commissioning of DARHT-2, one of the beam instabilities under study is ion-hose instability. The ion-hose instability is a transverse electrostatic instability which occurs as a result of the interaction between the beam and the ion channel transverse motions. In the previous study, the simulation of ion-hose instability in an induction accelerator was accomplished by a semi-analytical Spread Mass (SM) model or the particle-in-cell (PIC) code [2]. The aim of this work is to implement the SM model into Lamda [3], including varying axial magnetic field and beam acceleration and providing a fast and reliable simulation tool for DARHT operations.

In this paper, we describe the methods to incorporate the SM model into Lamda, and present benchmarking results against the SM code. To demonstrate the use of Lamda ion-hose calculation, two test cases using DARHT-2 configuration, a constant B_z case and an accelerating beam case, were carried out in comparison with PIC simulations.

*Work supported by Los Alamos National Laboratory

ION-HOSE INSTABILITY IN LAMDA

The motion of a particle due to the Lorentz force is determined by Newton's equation. In Lamda, by changing the dependent variable from t to z , we have the beam centroid equation

$$\gamma\beta^2\Delta\xi'' = -\gamma'\Delta x' + \frac{e}{mc^2}(E_x - \beta B_y + \beta\Delta y'B_z) \quad (1)$$

$$\gamma\beta^2\Delta y'' = -\gamma'\Delta y' + \frac{e}{mc^2}(E_y + \beta B_x - \beta\Delta x'B_z) \quad (2)$$

Δx and Δy are the centroid displacement of a particular beam slice in the x and y directions. γ and β are on axis values at the center of the beam. The external fields come from the accelerating gaps and the focusing solenoids. The transverse wall forces in a smooth beam pipe ($1/\gamma^2$ cancellation of electrical and magnetic forces) are also included in Eq. (1) and (2).

To incorporate SM model into the Lamda, we added an ion-term (the restoring force due to ions) in the existing beam centroid Eqs. (1) and (2). Modified beam centroid equations are written as:

$$\gamma\beta^2\Delta x'' = -\gamma'\Delta x' + \frac{e}{mc^2}(E_x - \beta B_y + \beta\Delta y'B_z) - 1.19\frac{2f_{ion}V_b}{a^2}(\Delta x - ion_x) \quad (3)$$

$$\gamma\beta^2\Delta y'' = -\gamma'\Delta y' + \frac{e}{mc^2}(E_y + \beta B_x - \beta\Delta x'B_z) - 1.19\frac{2f_{ion}V_b}{a^2}(\Delta y - ion_y) \quad (4)$$

The constant 1.19 comes from the SM model [2], which was originally described by Lee [4]. This constant is 1 for the rigid beam model. In the SM model, each longitudinal beam and ion slice consists of many rigid disks having different masses (equivalent to a spread in betatron frequencies). The $a = \sqrt{2}R_{rms}$ is the beam edge radius. The ion terms in Eq. 3 and 4 are the electrostatic force exerting on the beam due to the ion channel, which correspond to the $k_{\beta e}^2(b-d)$ term in the oscillation equation by Buchanan [5]. The ion_x and ion_y are the ion channel's positions in the x and y directions, respectively. We have created a subroutine, which was modified from the SM code, to calculate ion channel's position where the restriction of uniform beam and accelerator parameters are relaxed. This subroutine solves the SM version of equation of ion motion numerically.

The electrical and magnetic field, beam energy and radius are computed simultaneously with the ion-hose simulation in Lamda. There is no separated run or other transport code needed to obtain these parameters.

COMPARISON WITH SM CODE

To validate the SM model in Lamda, we used a uniform axial magnetic field case to benchmark Lamda against the SM code. The beam and accelerator parameters are given in Table 1. We assumed no acceleration in a 50 meter long draft tube. Therefore beam energy and beam radius were the constant along the distance of accelerator. Initial beam perturbation was given by a sinusoidal transverse displacement of amplitude 0.005 cm (the maximum of the beam offset allowed in the injector is 0.01 cm) at frequency of 21.6 MHz. This single frequency beam perturbation was used thoroughly in this work.

Table 1: Parameters for a constant B_z case.

Parameters	Values
Beam relativistic factor γ	25(12MeV)
Beam current	1.4 kA
Beam pulse length	2 μ s
Number of disk n_disk	2000
Beam rms radius	0.5 cm
Axial magnetic field	830 Gauss
Axial electric field	0
Transport distance	50 m
H ₂ O pressure	2×10^{-7} torr

The beam and ion channel displacements at the end of 50 m are plotted in Fig.1. The amplitude is in units of the beam rms radius R. Very good agreements between the Lamda and the SM code are seen for both ions and beam. Note that under uniform magnetic field and constant beam energy the physics models in Lamda and SM code are the same. However, their numerical integration methods are different, Lamda uses Runge-Kutta method and the SM code uses second order difference method. This might result in the discrepancy which increases with the time.

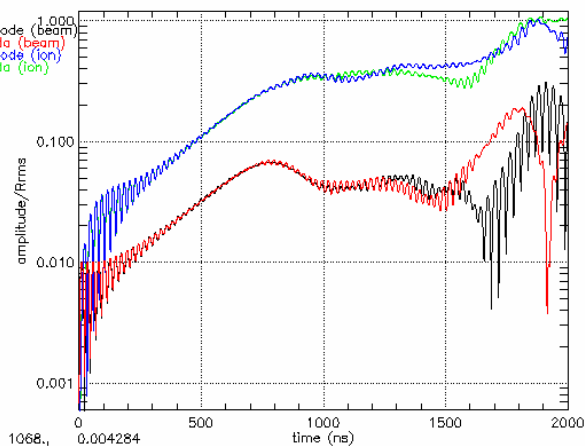


Figure.1: Amplitude of beam and ion channel from the SM code (beam-black, ions-blue) and Lamda calculations (beam-red, ions-green) using parameters in Table. 1.

Fig. 1 also shows that the ion-hose instability grows linearly in the early time and reaches to a saturated region

where the beam has become very nonlinear and the system falls out of resonance. The nonlinear effect slows down the instability.

The temporal resolution affects the Lamda calculation. In this work, we found that the accuracy of results requires $n_disk \geq 500$, i.e. the number of disks in an oscillation period is larger than 12.

COMPARISON WITH PIC CODE

Particle-in-cell code Lsp [6] has been used to check the ion-hose instability prediction of Lamda. For Lsp simulations, the transverse electric and magnetic fields are calculated from the magnetostatic approximation. Particles are pushed in the transverse direction using the Lorentz force. These treatments simplify the calculation. A typical running time with 4 machines is 24 ~ 48 hours.

Constant B_z , no Acceleration

The comparison of beam and ion centroids from Lamda and Lsp for a constant B_z case using parameters in Table 1 is presented in Fig. 2. For Lsp simulation, a normalized emittance of 0.1 cm-rad, which corresponds to a matched beam with the equilibrium beam radius $R_{rms} = 0.5$ cm, was used. Beam amplitude is calculated by $b = \sqrt{b_x^2 + b_y^2}$. We noticed that Lsp simulation using $dz=5$ cm gives an initial beam offset of ~ 0.01 cm, which is larger than the initial perturbation of 0.005 cm. In that case, the noise is larger than the real data. This noisiness is reduced significantly by using a smaller z-grid size of $dz = 2$ cm.

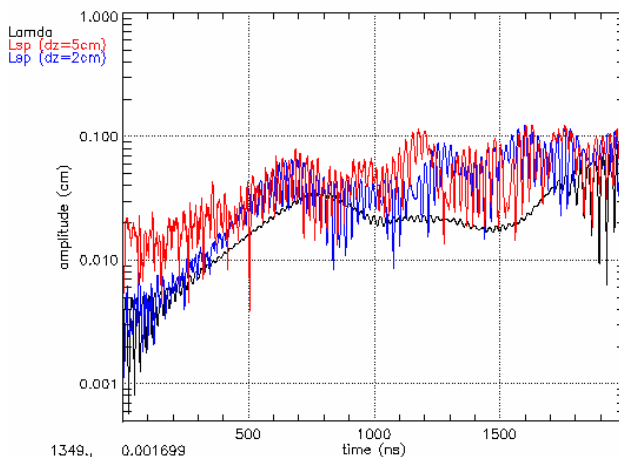


Figure 2: Comparison of beam centroid at end of 50-m drift tube, as calculated by Lamda (black), and Lsp using $dz = 5$ cm (red) and $dz = 2$ cm (blue) at a pressure of 2×10^{-7} torr for the constant B_z case.

The simulation comparison between Lsp and Lamda in Fig. 2 shows a good agreement overall. However, in the linear region, the growth rate (i.e. the slope in the diagram) from Lsp calculation is larger than the Lamda result. This could be due to different beam dynamic treatments in Lamda and Lsp. Lsp employs self-consistent

model of the beam and the SM model considers the beam as a collection of rigid disks. Other factors, such as the noisy in Lsp simulations, contribute to the difference too.

Accelerating Beams

This section we present ion-hose simulation comparison of Lamda and Lsp for an accelerating beam case. The beam was 1.4kA, 2.5-MV injector energy, a total of 56 cells with 6 injector cells (100kV each) and 50 accelerator cells (100kV each). A nominal tune for DARHT-2 long pulse experiments was used in simulations. For external electrical fields, we used a constant value by averaging the electrical fields of the accelerating gaps. For external magnetic fields, we used solenoid magnet data directly. The axial profile has large variation, as shown in Fig. 3. The axial grid size $dz = 2$ cm seems to resolve this structure well.

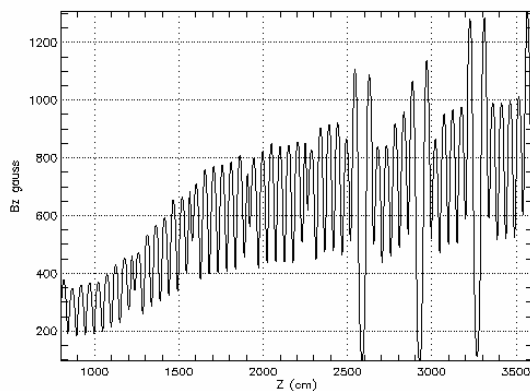


Figure 3: Axial magnetic field for an accelerating beam.

The simulations were carried out at two gas pressures, 2×10^{-7} torr and 1×10^{-6} torr. Comparison of beam and ion displacement at the exit of the accelerator $z = 3600$ cm calculated by Lsp and Lamda is presented in Fig. 4. As shown in Fig. 4a, the beam displacement after 2 μ s pulse is only about 5% of the beam radius at gas pressure of 2×10^{-7} torr. As the increase of gas pressure to 1×10^{-6} torr, significant evidence of ion-hose growth is seen in Fig. 4b. The simulation comparison in Fig. 4 shows a reasonable good agreement between Lamda and Lsp for an accelerating beam.

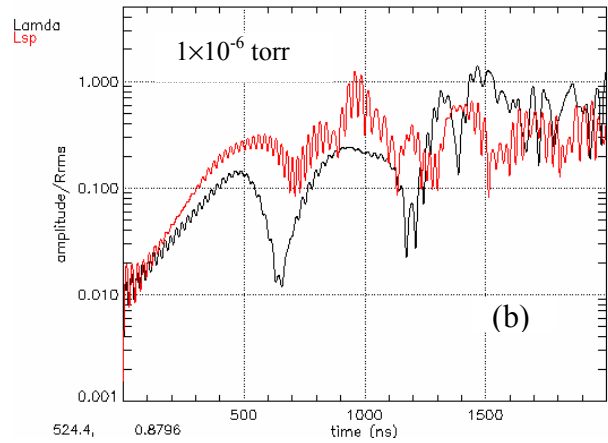
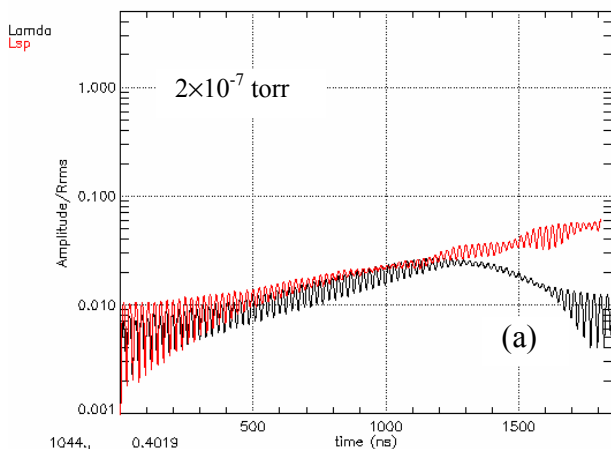


Figure 4: Amplitude of beam centroid at the exit of the accelerator from Lamda (black), and Lsp (red) at gas pressure of 2×10^{-7} torr (a) and 1×10^{-6} torr (b).

CONCLUSIONS

The SM model of ion-hose instability has been implemented in the Lamda code. The SM model in the Lamda is now capable of handling both the constant energy and accelerating beams. The Lamda code has been benchmarked against the SM code and the particle-in-cell code. Good agreements between Lamda, and the SM code and the PIC code are obtained. For an accelerating beam with a nominal tune for DARHT-2, Lamda results are consistent with the PIC code calculations. At gas pressure of 2×10^{-7} torr, ion-hose growth in the accelerator is not significant, but it is very evident at an increased gas pressure of 1×10^{-6} torr. The comparison results with Lsp show that Lamda code can predict ion-hose instability for DARHT with reasonable accuracy.

REFERENCES

- [1] C. Ekdahl, Jr., et al., "DARHT-II Long-Pulse Beam Dynamics Experiments", PAC'05, Knoxville, May 2005, p. 9.
- [2] T. C. Genoni and T. H. Hughes, "Ion-hose instability in a long-pulse linear induction accelerator", Phys. Rev. Special Topics-Accel. And Beams, Vol 6, 030401, 2003.
- [3] T. P. Hughes, et al., "LAMDA code for DARHT-2," Technical report MRC/ABQ-R-1428, July 2003.
- [4] E. P. Lee, Phys. Fluids, **21**, 1327, 1978.
- [5] H. L. Buchanan, Phys. Fluids, **30**, 221, 1987.
- [6] Lsp is a software product of ATK Mission Research Corporation, Albuquerque, NM 87110.